Journal of
Ceramic Science
and Technology

J. Ceram. Sci. Technol. 1-8 (2019)
DOI: 10.4416/JCST2019-00012
available online at: http://www.ceramic-science.com
© 2019 Göller Verlag

The Phase Composition and Mechanical Properties of Al_2O_3-TiN-TiC Ceramic Materials with Different Ni Content

Y. Fei*[1], Ch. Huang[2], H. Liu[3]

[1]College of Engineering, Qufu Normal University, Rizhao 276826, P. R. China No.80, Yantai Road, Donggang District, Rizhao, Shandong Province, P. R. China
[2]Center for Advanced Jet Engineering Technologies (CaJET), School of Mechanical Engineering, Shandong University, Jinan 250061, P. R. China No.17923, Jingshi Road, Lixia District, Jinan, Shandong Province, P. R. China
[3]Center for Advanced Jet Engineering Technologies (CaJET), School of Mechanical Engineering, Shandong University, Jinan 250061, P. R. China No.17923, Jingshi Road, Lixia District, Jinan, Shandong Province, P. R. China
received Febuary 12, 2019; received in revised form April 7, 2019; accepted June 18, 2019

Abstract

Research on the phase analysis of ceramic materials is less abundant than research on the microstructure. In this paper, Al_2O_3-TiN-TiC ceramic materials with different Ni content were fabricated by means of the hot-pressing technique. The effects of the content of Ni on the phase composition and the mechanical properties of sintered ceramic materials were investigated. The results showed that there were many diffraction peaks corresponding to the products of Ni in the range of 40°<2θ<45°, and the phases containing Ni element changed from spinel structure to intermetallic compounds. After sintering, many new phases appeared, such as Ti_8C_5, $TiC_{0.51}N_{0.12}$, $TiN_{0.90}$, $MgAl_2O_4$, Al_3Mg_2, and MoC. As the Ni content increased, both the flexural strength and the fracture toughness first increased then decreased, with the maximum values occurring when Ni content was 3 vol% However, the hardness decreased continuously as the Ni content increased. When the content of Ni was 3 vol%, the ceramic materials had optimum comprehensive mechanical properties at room temperature, the flexural strength, toughness and Vickers hardness reached 658.5 MPa, 7.0 MPa·m$^{1/2}$ and 19.8 GPa, respectively. The relationship between phase composition and the mechanical properties was also analyzed, and the phases beneficial to each of the three mechanical properties were obtained.

Keywords: Al_2O_3-TiN-TiC ceramic, Ni content, phase composition, mechanical properties

I. Introduction

High-speed machining technology is widely applied in the field of mechanical processing, owing to its high cutting speed and surface-machining accuracy [1–5]. The fabrication of cutting tools is one of the key technologies for high-speed machining. Al_2O_3 ceramic materials have been used for high-speed machining cutting tools for a long time. They are best suited for the high-speed machining of hard and brittle metal materials [6–10], such as chilled cast iron and hardened steel. The cutting conditions in high-speed machining demand excellent high-temperature and frictional wear performance of the cutting tools, which promotes the development of Al_2O_3-matrix ceramic materials. These materials usually contain additives that can improve mechanical properties such as strength, hardness, and toughness. The additives commonly used include reinforcing and toughening phases (e.g. TiC, SiC, TiN) [5–16], sintering aids (e.g. MgO, Y_2O_3) [17–20] and binding agents (e.g. Mo, Ni, Co) [21–26].

To date, many studies have been conducted on the effect of the secondary phases on the microstructure and mechanical properties of Al_2O_3-matrix ceramic materials. TiC [11,12] and TiN [11–15] are the most commonly used secondary phases of Al_2O_3-matrix ceramic materials. The melting temperature of TiC and TiN are 3 343 K and 3 203 K [22], respectively. Therefore, the composites exhibit good cutting performance for high-temperature and high-speed machining conditions [8–10] when TiC and TiN are introduced into alumina ceramics. Moreover, TiC particles improve the strength and hardness on account of the pinning effect on the crack front. Shalaby [5] investigated the wear mechanisms of several cutting tool materials in hard turning of high-carbon-chromium tool steel, concluding that Al_2O_3-TiC ceramic material is a chemically stable tool material with high red hardness and good toughness. TiN particles, on the other hand, reduce the friction coefficient, increase the hardness and improve the wear resistance. Al_2O_3-TiN ceramic materials exhibit better thermal shock stability and toughness than Al_2O_3-TiC ceramic materials. Moreover, TiN has excellent chemical stability and a low friction coefficient in contact with ferrous and Ni-based alloys, so it can be used as a wear-

* Corresponding author: yuhuanfei@qfnu.edu.cn

resistant component and cutting tool insert. The electrical conductivity of Al_2O_3-TiN material is 3.34×10^{-7} Ω·cm at room temperature, so the ceramic composite can be made by means of electrical discharge machining at low cost. The authors of this work have investigated Al_2O_3-TiN-TiC ceramic cutting tools for several years [9,10,15–18,21], and have shown that, with a proper composition of the starting material and appropriate sintering parameters, the ceramic cutting tools demonstrated better cutting performance than LT55 when cutting quenched steels.

Ni is one of the prominent metallic binding agents in brittle alumina matrix ceramic materials owing to its high ductility [23–33]. Verma *et al.* [27] mentioned that Ni could promote the densification of the composites via liquid phase sintering, and the relative density of the composites could be increased. Fahrenholtz *et al.* [28] demonstrated that Ni could enhance the fracture toughness of the composites through crack deflection and crack bridging. When the size of Ni particle is very small, the particles can slow down the mobility of the grain boundaries owing to the pinning mechanism, while a minimum amount of Ni addition can refine the Al_2O_3 matrix grains, and the strength of Al_2O_3 matrix is consequently enhanced [29–31]. As a result of the mismatch of the thermal expansion coefficient between Ni and Al_2O_3 [22,32], Ni addition can cause micro-crack and crack-bridging, which can improve the toughness.

In the field of materials research, the microstructure and its relationship with mechanical properties have always been the focus of research. Optical microscopy (OM), scanning electron microscopy (SEM), transmission electron microscopy (TEM) and other methods are used to observe the microstructure at different scales. In fact, the phase composition and phase structure also have significant impacts on the subsequent mechanical properties.

To date, the effect of adding Ni on alumina matrix ceramic materials has been mainly referred to the Al_2O_3-Ni system [23,24,26,28–30]. A lot of research has been done on the microstructure of this system, in order to ascertain the relationship between the microstructure and mechanical properties [23–26,28,29]. However, there are few investigations of the effect of Ni addition on the Al_2O_3-TiN-TiC material system. Meanwhile, it seems necessary to do more research to enable better understanding of the relationship between the phase composition and mechanical properties.

In this work, Al_2O_3-TiN-TiC ceramic materials with different Ni content were fabricated by means of the hot-pressing technique. The effects of the Ni content on the phase composition and mechanical properties were investigated. The relationship between different phases and the mechanical properties was also analyzed.

II. Experiments

(1) Starting materials and sample preparation

The physical properties and specifications of the raw materials are listed in Table 1 and Table 2, respectively. The Al_2O_3 powders are used as the matrix, TiC and TiN powders are selected to be the reinforcing and toughening additives. MgO powders are added as the sintering agent. Mo and Ni powders act as the metal binding additions. The average size of the α-Al_2O_3 matrix is 0.5 µm (purity: 99.9 %, Zibo, China), the average size of the TiC is 0.5 µm (purity: > 99 %, Hefei, China), the average size of the TiN is 0.5 µm (purity: > 99 %, Hefei, China), the average size of the MgO is 1.52 µm (purity: ≥ 98 %, Tianjin, China), the average size of the Ni is 2.3 µm (purity: ≥ 99.5 %, Beijing, China) and the average size of the Mo is 2.3 µm (purity: ≥ 99.7 %, Beijing, China).

The samples were prepared according to the following method: The powders were mixed using ethyl alcohol as the solvent, they were dispersed ultrasonically for 15 minutes using an SB5200 ultrasonic instrument and D-7401-III motor stirrer. Then the slurries were ball-milled with alumina balls for 48 hours to reduce the particle size and make the mixture more homogeneous. After that, a vacuum dry-type evaporator (Moder ZK-82A) was used to dry the mixture. The dried powders were passed through a 100-mesh sieve; then the powders were placed into a graphite die and were compacted by a jack. The final composites were fabricated by means of the hot-pressing technique in a ZRC85 – 25T sintering furnace, with an applied pressure of 32 MPa, a sintering temperature of 1 600 °C and the holding time of 10 minutes.

Four sets of samples were prepared, all of them had the same volume content of TiC (20 %), TiN (10 %), MgO (1 %), and Mo (1 %). The samples were distinguished from one another based on the composition of Ni, with the Ni volume content being 0 %, 1 %, 3 % and 5 %. For simplicity, the samples were named AC2UNi0, AC2UNi1, AC2UNi3, and AC2UNi5, respectively. Table 3 shows the composition of the four samples in this experiment. The preparation processes were repeated three times, with one set of samples being prepared each time.

Table 1: Physical properties of the raw materials [14]

Original phases	Density (g/cm³)	Melting point (°C)	Vickers hardness (GPa)	Elastic modulus (GPa)	Coefficient of thermal expansion (10^{-6}·K^{-1})	Poisson's ratio
Al_2O_3	3.98	2047	21	400	8.4	0.26
TiN	5.43	2930	20.7	590	9.3	0.22
TiC	4.93	3160	32	460	7.4	0.19
Ni	8.902	1453	0.638	197	13.3	0.31
Mo	10.2	2610	1.53	336	5.43	0.38
MgO	3.58	2852	0.91	208	13.8	0.18

Table 2: Specification information on the raw materials

Material	Purity	Average particle size (μm)	Density (g/cm3)	Manufacturer
Al_2O_3	99.9 %	0.5	3.99	Zibo, China
TiC	> 99 %	0.5	4.93	Hefei, China
TiN	> 99 %	0.5	5.43	Hefei, China
MgO	≥ 98 %	1.52	3.58	Tianjin, China
Mo	≥ 99.7 %	2.3	10.20	Beijing, China
Ni	≥ 99.5 %	2.3	8.90	Beijing, China

Table 3: Material composition and proportion (volume content).

No.	Al_2O_3	TiC	TiN	Ni	Mo	MgO
AC2UNi0	68 %	20 %	10 %	0	1%	1 %
AC2UNi1	67 %	20 %	10 %	1 %	1 %	1 %
AC2UNi3	65 %	20 %	10 %	3 %	1 %	1 %
AC2UNi5	63 %	20 %	10 %	5 %	1 %	1 %

(2) Characterization techniques

The sintered compacts were cut into bars with a diamond slice machine (J5060CE1), then the bars were ground and polished to obtain rectangular specimens with the size 4 mm × 3 mm × 30 mm. 4 ~ 5 bars could be obtained from each specimen. The room-temperature mechanical properties test was performed on a universal test machine (WDW-50E), the flexural strength of the materials was calculated in a three-point-bending test, with a span of 20 mm and a loading velocity of 0.5 mm/min. Two parts were obtained from the test of each bar. A Vickers-hardness-testing machine (HVS-50) was used to make an indention on the polished surface of the samples, with a load of 196 N and a loading holding time of 15 seconds. 2 ~ 3 indentions were obtained from the separated bars after the three-point-bending test. Then, the Vickers hardness and fracture toughness of the materials were calculated with the direct indentation method.

The phase composition of the sintering body was determined by means of X-ray diffraction (XRD) on a diffractometer (D/max-rb) with copper Kα radiation. The typical microstructures of the polished and fracture surfaces were observed by means of SEM with energy-dispersive spectrometry (ZEISS SUPRA-55). Both XRD and SEM were applied on at least three specimens. Line scanning, area scanning and EDS (Energy-Dispersive Spectrometer) were applied for each specimen.

III- Results and Discussion

(1) Phase composition

Fig. 1 shows the X-ray diffraction results of the samples. Fig. 1e) is the comparison diagram, it indicates that with the addition of Ni, there are more diffraction peaks in the range of 2θ=40°~45° and the new diffraction peaks become stronger with the increment of Ni content. The phase identification indicates that these diffraction peaks are attributed to Ni contributions.

Table 4 shows the details of the consequent phase composition of the specimens.

Firstly, it can be seen that all the specimens have the Al_2O_3 phase with the same lattice structure.

Secondly, when the content of Ni is less than 5 vol%, TiC is transformed into Ti_8C_5 (rhombohedral system) and TiN is transformed into osbornite-TiN (cubic system). When the Ni content is 5 vol%, TiC and TiN dissolve completely and generate $TiC_{0.51}N_{0.12}$ (hexagonal system), while the remaining TiN is changed to $TiN_{0.90}$ (cubic system). Ti_8C_5 has been observed in the Ni-Ti-C system 32. Additionally, the research of Rotella *et al.* 34 have indicated that Ti_8C_5 is more porous and has slightly different properties from TiC. $TiC_{0.51}N_{0.12}$ is one kind of TiC_xN_y phase. It is known that, when the sum of x and y is equal or close to one, the mechanical properties of the ceramic materials are excellent. However, when the sum of x and y is less than one, the excess Ti elements and the liquid phase generate brittle phase, which reduces the strength of ceramic materials.

Thirdly, the addition of MgO leads to two kinds of the $MgAl_2O_4$ phases, one is the spinel of the cubic system and the other is the orthorhombic system. When there is no Ni addition in the initial powders, the $MgAl_2O_4$ phase of orthorhombic system structure is the dominant form. When the Ni content is 1 vol%, MgO in the initial powders turns into Al_3Mg_2 (cubic system) with a large volume expansion. When the Ni content is 3 vol%, MgO in the initial powders turns into $MgAl_2O_4$ of the cubic system with a smaller cell volume; the volume change could make the density higher, which would be beneficial to the desired mechanical properties. When the Ni content is 5 vol%, MgO also exists in the $MgAl_2O_4$ phase of the cubic system. Different lattice structure and cell volume cause different density, which can affect the properties of the phase.

There is a host of literature 35 – 37 investigating Al_3Mg_2 (β-Samson) because of its special crystal structure feature, which is called "one of the most complicated crystal structures in intermetallic compounds of alloys", but the relationship between structure and properties is still an unanswered question. Kim *et al.* 38 and Huang *et al.* 39 concluded that $MgAl_2O_4$ could control the transfer rate of grain-boundaries, which is beneficial to the microstructure and mechanical properties of ceramic composites.

Moreover, the addition of Mo leads to the interstitial phase MoC (cubic system) when there is no Ni addition in the initial powders. When the Ni content is 1 vol%, Mo element exists in the form of MoC (hexagonal system) and the cell volume becomes bigger. When the Ni content is 3 vol%, Mo exists in the form of $Al_{12}Mo$ (cubic system) and the cell volume is bigger than hcp-MoC. When the Ni content reaches 5 vol%, Mo exists in the form of MoC (cubic system) again.

Last but not least, when the Ni content is 1 vol%, Ni element exists in the form of $NiAl_2O_4$ (cubic system), so-called spinel. Konopka *et al.* [40] indicated that the branching cracks by $NiAl_2O_4$ spinel particles could improve the fracture toughness of Al_2O_3-Ni composites. Konopka *et al.* [41 – 42] also concluded that a small amount of $NiAl_2O_4$ spinel formation was beneficial to crack bridging. When the Ni content is 3 vol%, Ni element and Al element generate $Al_{0.9}Ni_{3.22}$ (cubic system). The lattice structure of

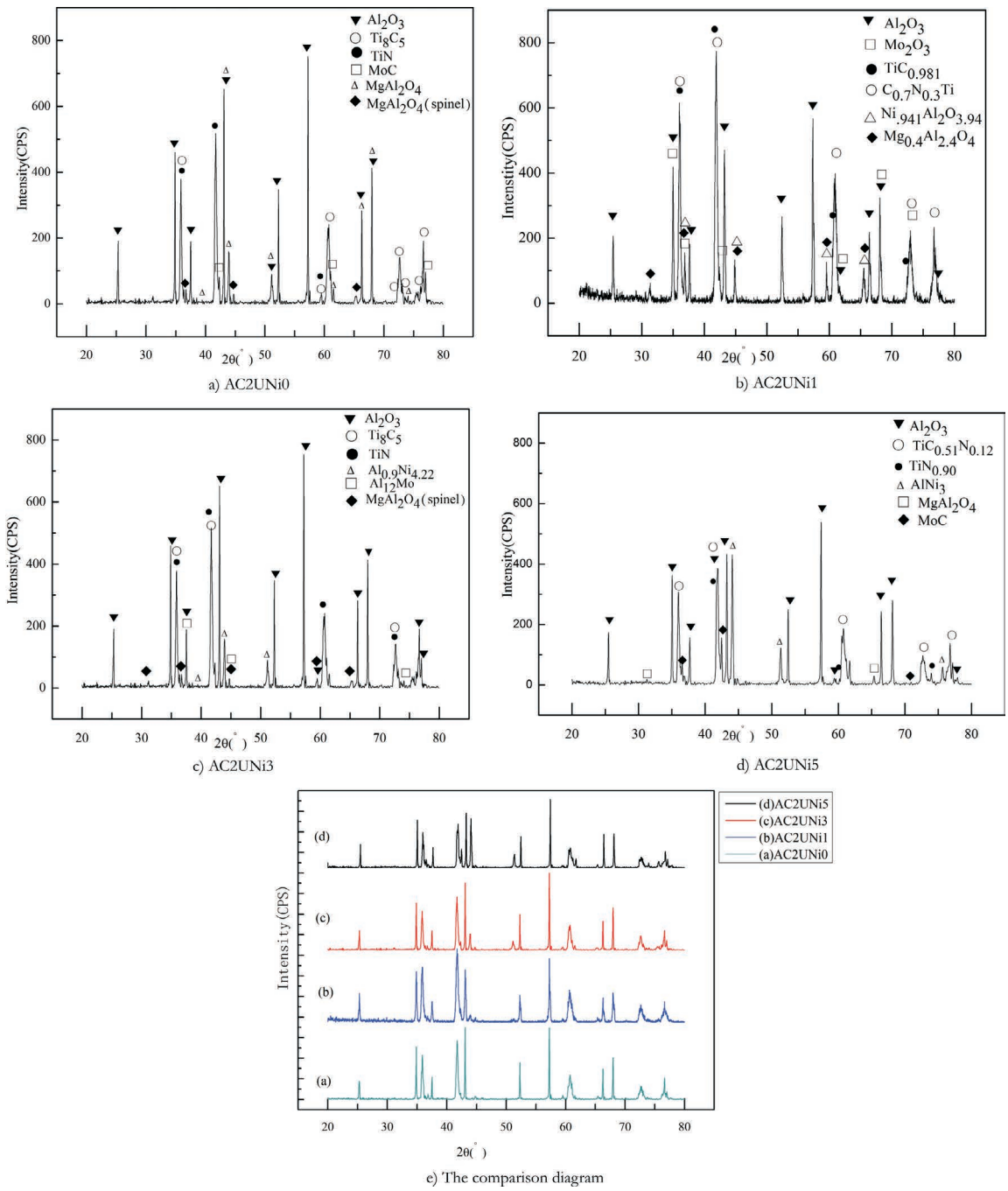

Fig. 1: X-ray diffraction patterns of the Al_2O_3-TiC-TiN-Mo-MgO samples with 0 a), 1 b), 3 c) and 5 d) vol% Ni additions and their comparison e).

Table 4: Phase composition of Al_2O_3-TiN-TiC ceramic materials with different Ni content.

No.	Al_2O_3	TiC	TiN	Mo	Ni	MgO
AC2UNi0	Al_2O_3	Ti_8C_5 (rhombohedral)	osbornite-TiN (cubic)	MoC (cubic)	—	$MgAl_2O_4$ (cubic)
AC2U	Al_2O_3	Ti_8C_5 (rhombohedral)	osbornite-TiN (cubic)	MoC (hexagonal)	$NiAl_2O_4$ (cubic)	Al_3Mg_2
AC2UNi3	Al_2O_3	Ti_8C_5 (rhombohedral)	osbornite-TiN (cubic)	$Al_{12}Mo$	$Al_{0.9}Ni_{3.22}$	$MgAl_2O_4$ (orthorhombic)
AC2UNi5	Al_2O_3	$TiC_{0.51}N_{0.12}$ (hexagonal)	$TiN_{0.90}$ (cubic)	MoC (cubic)	Ni_3Al	$MgAl_2O_4$ (orthorhombic)

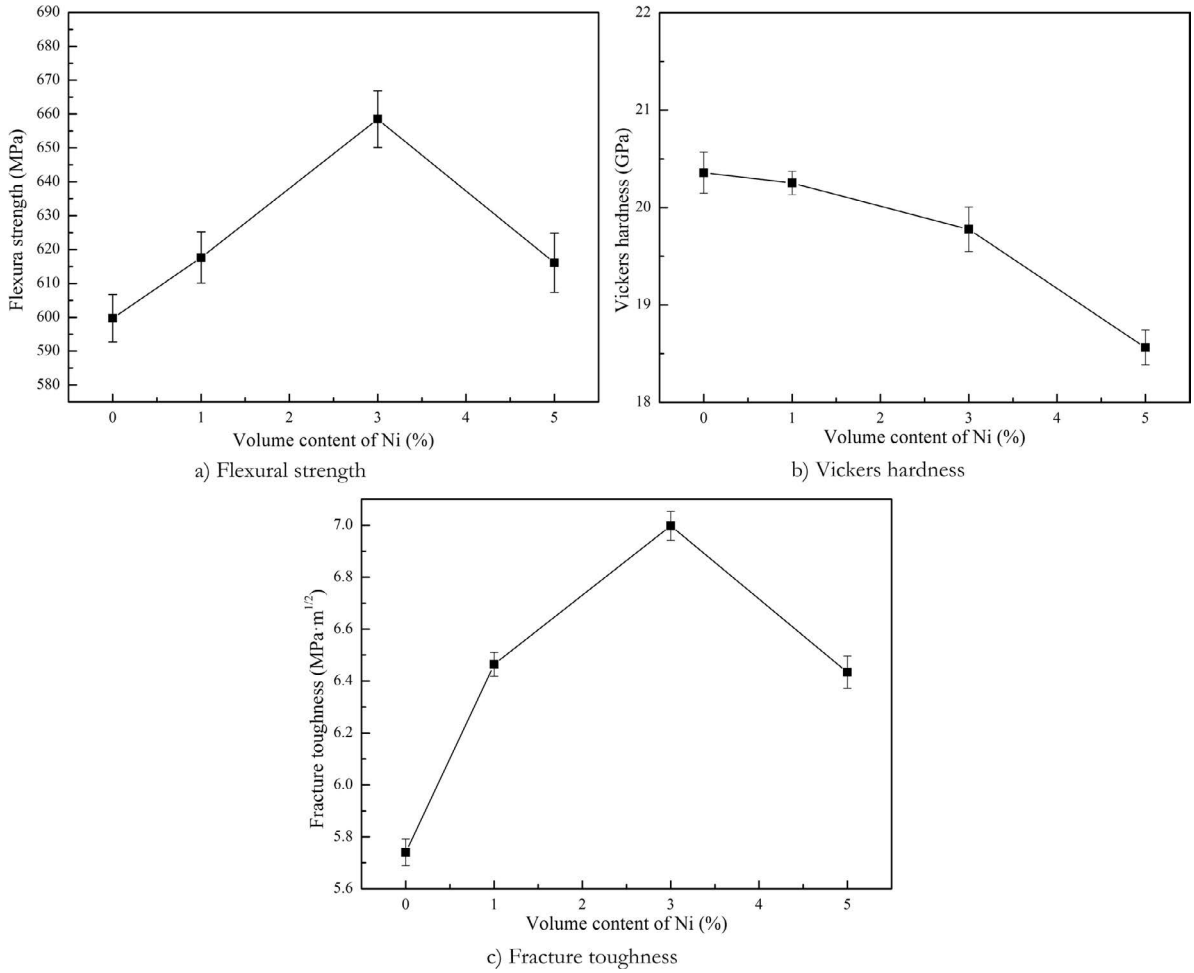

Fig. 2: The mechanical properties of the ceramic materials with different Ni additions, in which a) is the flexural strength, b) is the Vickers hardness and c) is the fracture toughness.

$Al_{0.9}Ni_{3.22}$ is the same as that of Ni_3Al, but the non-stoichiometric features will cause the point defects of antisite defects. When there is surplus Ni, Ni anti-position defects tend to maintain $L1_2$ structure [43–44], which can improve the strength and toughness of the materials. When the Ni content is 5 vol%, Ni and Al elements generate intermetallic compound Ni_3Al and the diffraction peak of $Ni_3Al$is strong. Most intermetallic compounds are hard and brittle [45–46], so the mechanical properties of ceramic materials will be poor when there are too many intermetallic compounds.

(2) Mechanical properties

Fig. 2 illustrates the effects of Ni content on the mechanical properties of Al_2O_3-TiN-TiC ceramic materials. The results from previous work [9, 10] suggest that they all have ideal mechanical properties, which makes them good candidates for use as cutting tools, enabling them to be used to cut quenched steels.

From Fig. 2b), it can be seen that with the increment of the Ni content, the Vickers hardness decreases continuously and quickly. This can be explained by the fact that the inherent hardness of Ni (0.7 GPa) is lower than that of

the Al_2O_3 matrix (21 GPa) and the additives TiC (32 GPa) and TiN (20.7 GPa). As indicated in Fig. 2a) and Fig. 2c), the flexural strength and the fracture toughness change in the same way. When there is no Ni, both of these reach the minimum values. With the increment of Ni content, both the flexural strength and the fracture toughness increase up to a maximum value and then decrease. When the Ni content is 3 vol%, the flexural strength and the fracture toughness reach the maximum values.

To sum up, when the Ni content is 3 vol%, the comprehensive mechanical properties of the ceramic materials are the best, the flexural strength is 658.5 MPa, the Vickers hardness is 19.8 GPa and the fracture toughness is 7.0 MPa·m$^{1/2}$.

Fig. 3 shows typical SEM results of AC2UNi3.

Fig. 3a) shows that there are various core-shell structures in AC2Ni3 (as marked by the red circles). Fig. 3b) shows the line scanning photos of Fig. 3a), the results indicate that the bright white part in Fig. 3a) is the binding phase generated by Ni and the light grey part in Fig. 3a) is the hard phase TiC. The wetting angles of Ni with Al_2O_3 and TiC are 128°and 30°, respectively 46. As a consequence, liquid Ni can wet TiC much better than Al_2O_3 during the sintering process, therefore the Ni products distribute around hard phase in the sintered body. The various core-shell structures indicate that the hard phase is sufficiently wetted by Ni particles, which could enhance the mechanical properties.

Fig. 3c) is the topography on the polished surface of AC2Ni3 and Fig. 3d) is the topography on the polished surface of AC2Ni3. Fig. 3c) shows that Ni production is more dispersed, and the particle size is bigger at the grain boundary than inside the grain. The dispersion at the grain boundary can restrain crack propagation, which can improve the fracture toughness of the material [47]. On the other hand, the small particles distributed in Al_2O_3 matrix can improve the density of the material. As indicated in Fig. 3d), there are both intergranular fracture and transgranular fracture in the fracture surface, and the fracture morphologies are mainly transgranular fracture, thereby enhancing the fracture toughness. The grains are uniform, and the grain size is small, which could improve the strength and hardness according to the Hall-Patch relationship.

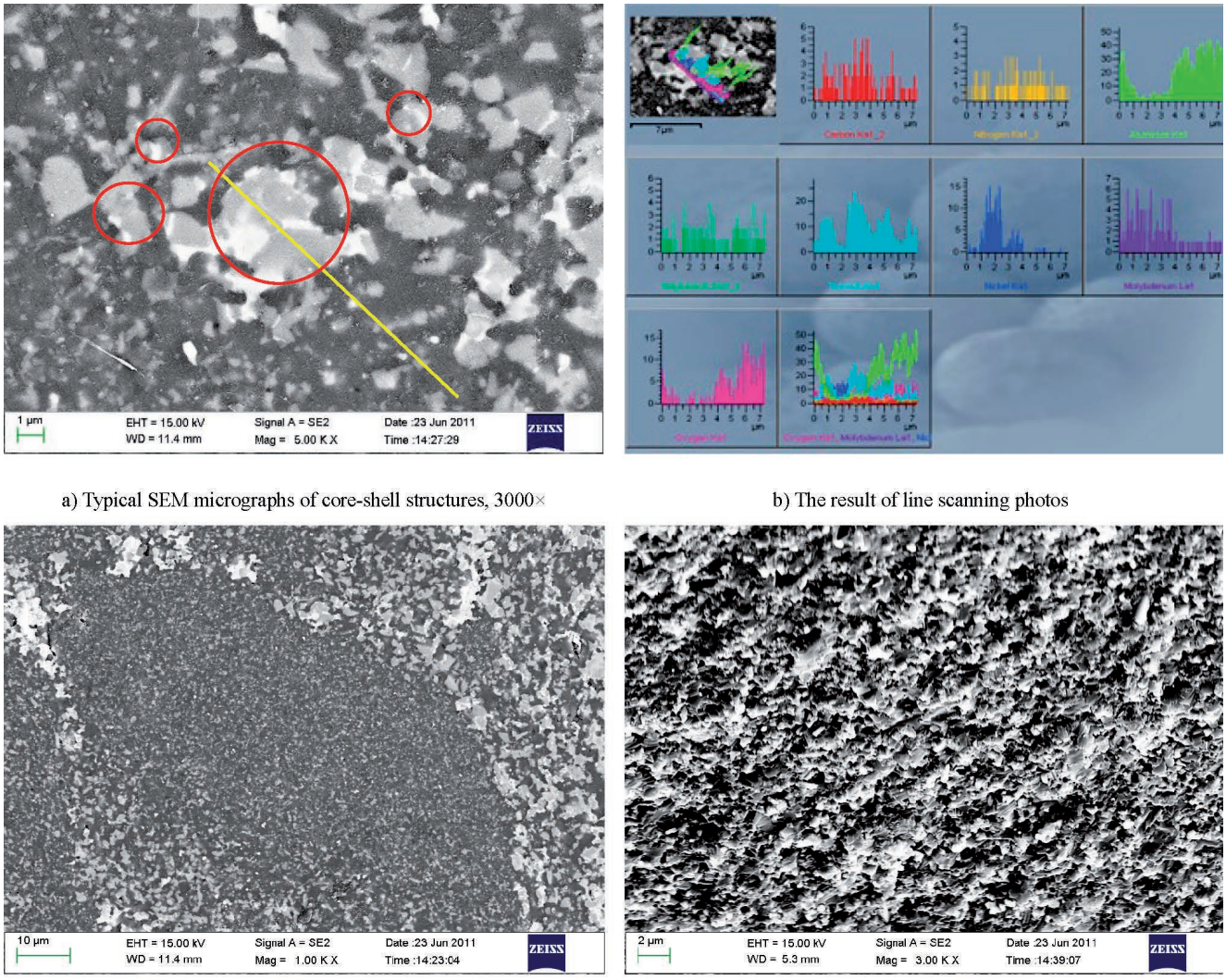

a) Typical SEM micrographs of core-shell structures, 3000×

b) The result of line scanning photos

c) SEM micrographs of the polished surfaces, 1000×

d) SEM micrographs of the fracture surfaces, 3000×

Fig. 3: SEM results of AC2UNi3 [17], in which a) shows the typical core-shell structures, b) shows the line scanning photos of a), c) shows the micrographs of the polished surface and d) shows the micrographs of the fracture surfaces.

(3) The relationship between different phases and mechanical properties

In a comparison of the phase composition with mechanical properties, the relationship between some phases and specific mechanical properties can be found. The relationship between certain phases with specific mechanical properties can be inferred from Table 4 and Fig. 2.

When Mg element exists in the form of orthorhombic-$MgAl_2O_4$, the flexural strength of the ceramic materials is worst (599.7 MPa), which means spinel-$MgAl_2O_4$ and Al_3Mg_2 can improve the flexural strength of Al_2O_3-TiN-TiC ceramic materials. When the Ni content is 3 vol%, the flexural strength and fracture toughness reach the maximum values (658.5 MPa and 7.0 MPa·m1/2, respectively), which means that the generated phases $Al_{0.9}Ni_{3.22}$ and $Al_{12}Mo$ can improve the flexural strength and fracture toughness. All mechanical properties decrease when the Ni content increases to 5 vol%, it can be concluded that the generated phases $TiN_{0.90}$ and $TiC_{0.51}N_{0.12}$ cause the decrease in the comprehensive properties. This conclusion is in agreement with the analysis and discussion of the specific phases in the first part of the Results and Discussion.

IV. Conclusions

The addition of Ni can improve flexural strength and fracture toughness, but reduces hardness. With sintering process parameters of 1 600 °C, 32 MPa and 10 minutes holding time, the best comprehensive mechanical properties are obtained when the Ni content is 3 vol%. The flexural strength, Vickers hardness, and fracture toughness are 658.5 MPa, 19.8 GPa and 7.0 MPa·$m^{1/2}$, respectively.

With the increment of Ni content, the Ni element in the ceramic materials causes a change from spinel structure ($NiAl_2O_4$, with the Ni content of 1 vol%) to intermetallic compounds ($Al_{0.9}Ni_{3.22}$ and Ni_3Al, with the Ni content of 3 vol% and 5 vol%, respectively), which reduces the hardness owing to the defect of intermetallic compounds. Orthorhombic-$MgAl_2O_4$ is not desirable for the flexural strength of the Al_2O_3-TiN-TiC ceramic materials. The generated phases $Al_{0.9}Ni_{3.22}$ and $Al_{12}Mo$ can improve the flexural strength and fracture toughness, whereas the existence of $TiN_{0.90}$ and $TiC_{0.51}N_{0.12}$ causes a decrease in the comprehensive properties.

Acknowledgement

This work was supported by National Natural Science Foundation of China (Grant No. 51705286, 51675313), Natural Science Foundation of Shandong Province (Grant No. ZR2017BEE057, ZR2014EEM013), the Opening Laboratory Fund of Qufu Normal University (Grant No. SK201516), and the Scientific Research Foundation of Qufu Normal University (Grant No. BSQD20131426).

Availability of data and materials

The data sets supporting the conclusions of this article are included in the article.

Competing interests

The authors declare no competing financial interests.

Ethics approval and consent to participate

Not applicable.

References

1 Tu, G.Z., Wu, S.H., Liu, J., Long, Y., Wang, B.: Cutting performance and wear mechanisms of sialon ceramic cutting tools at high speed dry turning of gray cast iron, *Int. J. Refract. Met.*, **54**, 330 – 334, (2016).

2 D'Mello, G., Pai, P.S., Puneet, N.P.: Optimization studies in high speed turning of Ti-6Al-4V, *App. Soft. Comput.*, **51**, 105 – 115, (2017).

3 Kar, S., Bandyopadhyay, P.P., Paul, S.: High speed and precision grinding of plasma sprayed oxide ceramic coatings, *Ceram. Int.*, **43**, 15316 – 15331, (2017).

4 Obikawa, T., Yamaguchi, M.: Suppression of notch wear of a whisker reinforced ceramic tool in air-jet-assisted high-speed machining of inconel 718, *Precis. Eng.*, **39**, 143 – 151, (2015).

5 Shalaby, M.A., Hakim, M.A.E., Abdelhameed, M.M., Krzanowski, J.E., Veldhuis, S.C., Dosbaeva, G.K.: Wear mechanisms of several cutting tool materials in hard turning of high carbon-chromium tool steel, *Tribol. Int.*, **70**, 148 – 154, (2014).

6 Liu, X.F., Liu, H.L., Huang, C.Z., Wang, L.M., Zou, B., Zhao, B.: Synergistically toughening effect of SiC whiskers and nanoparticles in Al_2O_3-based composite ceramic cutting tool material, *Chin. J. Mech. Eng-En.*, **29**, [5], 977 – 982, (2016).

7 Kumar, C.S., Patel, S.K.: Hard machining performance of PVD AlCrN coated Al_2O_3/TiCN ceramic inserts as a function of thin film thickness, *Ceram. Int.*, **43**, [16],13314 – 13329, (2017).

8 Wang, D., Xue, C., Cao, Y., Zhao, J.: Fabrication and cutting performance of an Al_2O_3/TiC/TiN ceramic cutting tool in turning of an ultra-high-strength steel, *Int. J. Adv. Manuf. Tech.*, **91**, 1967 – 1976, (2017).

9 Fei, Y.H., Huang, C.Z., Liu. H.L., Zou, B.: Study on the cutting performance of Al_2O_3-TiC-TiN ceramic tool materials, *Key Eng. Mater.*, **40**, 10205 – 10209, (2016).

10 Fei, Y.H., Huang, C.Z., Liu, H.L., Zou, B.: Study on the cutting performance of the novel Al_2O_3-matrix ceramic cutting tools in turning quenched 40Cr, (in Chinese), *Tool Engineering*, **40**, 10205 – 10209, (2018).

11 Meir, S., Kalabukhov, S., Hayun, S.: Low temperature spark plasma sintering of Al_2O_3-TiC composites, *Ceram. Int.*, **40**, 12187 – 12192, (2014).

12 Yin, Z.B., Huang, C.Z., Zou, B., Liu, H.L., Zhu, H.T., Wang, J.: Study of the mechanical properties, strengthening and toughening mechanisms of Al_2O_3/TiC micro-nano-composite tool materials, *Mat. Sci. Eng. A.*, **577**, 9 – 15, (2013).

13 Qiao, L.N., Zhao, Y.C., Wang, M.Z., Shi, C.J., Ye, Y.N., Zhang, J.X., Zou, Q., Yang, Q., Deng, H., Xing, Y.: Enhancing the sinterability and fracture toughness of Al_2O_3-$TiN_{0.3}$ composites, *Ceram. Int.*, **42**, 3965 – 3971, (2016).

14 Li, J.G., Gao, L., Guo, J.K.: Mechanical properties and electrical conductivity of TiN-Al_2O_3 nanocomposites, *J. Eur. Ceram. Soc.*, **23**, 69 – 74, (2003).

15 Fei, Y.H., Huang, C.Z., Liu, H.L., Zou, B.: Mechanical properties of Al_2O_3-TiN nanocomposite ceramic tool materials, *Key Eng. Mater.*, **499**, 108 – 113, (2012).

16 Fei, Y.H., Huang, C.Z., Liu, H.L., Zou, B.: Mechanical properties of Al_2O_3-TiC-TiN ceramic tool materials, *Ceram. Int.*, **40**, 10205 – 10209, (2014).

17 Fei, Y.H., Huang, C.Z., Liu, H.L., Zou, B.: The influence of Ni addition on the mechanical properties and microstructures of Al_2O_3-TiC-TiN ceramic tool materials, *Nanomanufacturing and Metrology*, **1**, [2], 105 – 111, (2018).

18 Fei, Y.H., Huang, C.Z., Liu, H.L., Zou, B.: The effect of MgO content on the mechanical properties and microstructures of Al_2O_3-TiN-TiC ceramic materials, *Adv. Mater. Res.*, **500**, 623 – 628, (2012).

19 Laine, R.M., Taylor, N.J., Stangeland-Molo, S.: Processing YAG/α-Al_2O_3 composites via reactive sintering Y_2O_3/Al_2O_3 NP mixtures: A superior alternative to bottom up processing using atomically mixed $YAlO_x$ NPs, *J. Am. Ceram. Soc.*, **100**, [10], 4500 – 4510, (2017).

20 Luo, J.M., Xu, J.L.: Y_2O_3-doped Al_2O_3 transparent ceramics prepared by low temperature microwave sintering. In Proceedings of the 5th International Conference on Advanced Design and Manufacturing Engineering. Shenzhen, China, 2015.

21 Fei, Y.H., Huang, C.Z., Liu, H.L., Zou, B.: The effects of Mo addition on the microstructures and mechanical properties of Al_2O_3-TiN-TiC ceramic materials, (in Chinese), Modular machine tool & automatic manufacturing technique, [08], 23 – 27, (2012).

22 Li, R.J.: Ceramic-metal composites, (in Chinese),1st edition. Metallurgy Industry Press, Beijing, 32 – 86, 1995.

23 Yang, S., Kim, H., Lee, C.S.: Investigation of shrinkage control in Ni-Al_2O_3 (Metal-Ceramic) functionally graded materials, *Ceram. Int.*, **39**, [1], 93 – 99, (2013).

24 Li, G.J., Huang, X.X., Guo, J.K.: Fabrication and mechanical properties of Al_2O_3-Ni composite from two different powder mixtures, *Mat. Sci. Eng. A.*, **352**, $^{1-2}$, 23 – 28, (2003).

25 Kumar, R., Chaubey, A., Maity, T., Prashanth, K.G.: Mechanical and tribological properties of Al_2O_3-TiC composite fabricated by spark plasma sintering with metallic (Ni, Nb) binders, *Metals*, **8**, [1], 1 – 12, (2018).

26 Lu, J.S., Gao, L., Sun, J., Gui, L.H., Guo, J.K.: Effect of nickel content on the sintering behavior, mechanical and dielectric properties of Al_2O_3/Ni composites from coated powders, *Mat. Sci. Eng. A.*, **293**, [1 – 2], 223 – 228, (2000).

27 Verma, V., Kumar, B.V.M.: Synthesis, microstructure and mechanical properties of $Al_2O_3/ZrO_2/CeO_2$ composites with addition of nickel and titania processed by conventional sintering, *Mater. Today.:*, **4**, [2] A, 3062 – 3071, (2017).

28 Fahrenholtz, W.G., Ellerby, D.T., Loehman, R.E.: Al_2O_3-Ni composites with high strength and fracture toughness, *J. Am. Ceram. Soc.*, **83**, [5], 1279 – 1280, (2004).

29 Sun, X.D., Yeomans, J.A.: Microstructure and fracture toughness of nickel particle toughened alumina matrix composites, *J. Mater. Sci.*, **31**, [4], 875 – 880, (1996).

30 Tuan, W.H., Chen, J.R., Yang, T.J.: Minimum amount of nanosized nickel particles to enhance the strength of alumina, *J. Eur. Ceram. Soc.*, **27**, [16], 4705 – 4709, (2007).

31 Golonka, A., Moskała, N., Putyra, P., Pyda, W.: Effects of nano-nickel and MgO addition to alumina based matrices on properties of the resultant composites, *Ceram. Mater.*, **66**, [2],175 – 184, (2014).

32 Hattali, L., Stéphane, V., Ropital, F., Mesrati, N., Tréheux, D.: Effect of thermal residual stresses on the strength for both alumina/Ni/alumina and alumina/Ni/nickel alloy biomaterials, *J. Mater. Sci.*, **44**, [12], 3198 – 3210, (2009).

33 Zhu, G, Wang, W., Wang, R., Zhao, C., Pan, W., Huang, H., Du, D., Wang, D., Shu, D., Dong, A., Sun, B., Jiang, S., Pu, Y.: Formation mechanism of spherical TiC in Ni-Ti-C system during combustion synthesis, *Materials (Basel)*, **10**, [9], 1007, (2017).

34 Rotella, C., Hettinger, J.D., Cortes, E., Lofland, S.E., Heon, M., Lunk, C.: Properties of Ti_8C_5 thin films created at different temperatures using magnetron sputtering. In American Physical Society, APS March Meeting. Baltimore, USA, 2013.

35 Feuerbacher, M., Thomas C., Makongo, J.P.A., *et al.*: The samson phase, β-Al_3Mg_2, revisited, *Z. Krist. – Crysta. Mater.*, **222**, [6], 259 – 288, (2007).

36 Nakayama, K., Tsuruta, H., Koyama, Y.: Formation of giant atomic clusters in the β-samson (β-Al_3Mg_2) phase of the al-mg alloy system, *Acta. Mater.*, **128**, 249 – 257, (2017).

37 Straumal, B.B., Kogtenkova, O.A., Murashkin, M.Y., Bulatov, M.F., Czeppe, T., Zięba, P.: Grain boundary wetting transition in al-mg alloys, *Mater. Lett.*, **186**, 82 – 85, (2017).

38 Kim, B., Hong, S., Lee, S., Kim, D., Hwang, N.: Alternative explanation for the role of magnesia in the sintering of alumina containing small amounts of a liquid phase, *J. Am. Ceram. Soc.*, **86**, [4], 634 – 639, (2003).

39 Huang, S.S., Zhou, W.W., Luo, F., Wei, P., Zhu, D.M.: Mechanical and dielectric properties of short carbon fiber reinforced Al_2O_3 composites with MgO additive, *Ceram. Int.*, **40**, 2785 – 2791, (2014).

40 Konopka, K., Miazga, A., Właszczuk, J.: Fracture toughness of Al_2O_3-Ni composites with nickel aluminate spinel phase $NiAl_2O_4$, *Compos.*, **11**, [7], 197 – 201, (2011).

41 Konopka, K.: Nickel aluminate spinel ($NiAl_2O_4$) in Al_2O_3-Ni composite, *Mater. Eng.*, **31**, [3], 457 – 459, (2010).

42 Konopka, K., Zygmuntowicz, J., Miazga, A.: Morphology of nickel aluminate spinel ($NiAl_2O_4$) formed in the Al_2O_3-Ni composite system sintered in air, *Composites, Theor. Pract.*, **14**, [2], 106 – 110, (2014).

43 Yu, S., Wang, C.Y., Yu, T.: Study of the point defect, resite, and recluster in reembedded Ni_3Al using the embedded atom method, (in Chinese), *Acta. Phys. Sin.*, [6], 3212 – 3218, (2007).

44 Shi, D.M., Wen, B., Melnik, R., Yao, S., Li, T.J.: First-principles studies of Al-Ni intermetallic compounds, *J. Solid. State. Chem.*, **182**, [10], 2664 – 2669, (2009).

45 Rzyman, K., Moser, Z.: Calorimetric studies of the enthalpies of formation of Al_3Ni_2, AlNi and $AlNi_3$, *Prog. Mater. Sci.*, **49**, [1 – 2], 581 – 606, (2004).

46 Li, Q., Sun, X.D., Xiu, Z.M.: Effect of Ni and Ti on mechanical properties of Al_2O_3-Ti(C, N) composites, (in Chinese), *J. Inorg. Mater.*, **26**, [9], 955 – 960, (2011).

47 Li, G.J., Chen, D.M., Huang, X.X., Guo, J.K.: Effect of residual thermal stresses on fracture behavior and mechanical properties of Al_2O_3/Ni cermets, (in Chinese), *J. Mater. Eng.*, **12**, 36 – 38, (2002).